

A planetary system around the nearby M dwarf GJ 667C with at least one super-Earth in its habitable zone.

Guillem Anglada-Escudé^{1,2}, Pamela Arriagada³, Steven S. Vogt⁴, Eugenio J. Rivera⁴, R. Paul Butler¹, Jeffrey D. Crane⁵, Stephen A. Slichtman⁵, Ian B. Thompson⁵, Dante Minniti^{3,6,7}, Nader Haghighipour⁸, Brad D. Carter⁹, C. G. Tinney¹⁰, Robert A. Wittenmyer¹⁰, Jeremy A. Bailey¹⁰, Simon J. O'Toole¹¹, Hugh R.A. Jones¹², James S. Jenkins¹³

anglada@dtm.ciw.edu

ABSTRACT

We re-analyze 4 years of HARPS spectra of the nearby M1.5 dwarf GJ 667C available through the ESO public archive. The new radial velocity (RV) measurements were obtained using a new data analysis technique that derives the Doppler measurement and other instrumental effects using a least-squares approach. Combining these new 143 measurements with 41 additional RVs from

¹Carnegie Institution of Washington, Department of Terrestrial Magnetism, 5241 Broad Branch Rd. NW, Washington D.C., 20015, USA

²Universität Göttingen, Institut für Astrophysik, Friedrich-Hund-Platz 1, 37077 Göttingen, Germany

³Department of Astronomy, Pontificia Universidad Católica de Chile, Casilla 306, Santiago 22, Chile

⁴UCO/Lick Observatory, University of California, Santa Cruz, CA 95064, USA

⁵Carnegie Observatories, 813 Santa Barbara St., Pasadena, CA 91101-1292, USA

⁶Vatican Observatory, V00120 Vatican City State, Italy

⁷Department of Astrophysical Sciences, Princeton University, Princeton NJ 08544-1001

⁸Institute for Astronomy & NASA Astrobiology Institute, University of Hawaii-Monoa, 2680 Woodlawn Drive, Honolulu, HI 96822, USA

⁹Faculty of Sciences, University of Southern Queensland, Toowoomba, 4350, Australia

¹⁰Department of Astrophysics, School of Physics, University of New South Wales, Sydney 2052, Australia

¹¹Australian Astronomical Observatory, PO Box 296, Epping, 1710, Australia

¹²Centre for Astrophysics Research, University of Hertfordshire, College Lane, Hatfield, Herts, AL10 9AB, UK

¹³Departamento de Astronomía, Universidad de Chile, Camino El Observatorio 1515, Las Condes, Santiago, Chile

the Magellan/PFS and Keck/HIRES spectrometers, reveals 3 additional signals beyond the previously reported 7.2-day candidate, with periods of 28 days, 75 days, and a secular trend consistent with the presence of a gas giant (Period \sim 10 years). The 28-day signal implies a planet candidate with a minimum mass of $4.5 M_{\oplus}$ orbiting well within the canonical definition of the star’s liquid water habitable zone, this is, the region around the star at which an Earth-like planet could sustain liquid water on its surface. Still, the ultimate water supporting capability of this candidate depends on properties that are unknown such as its albedo, atmospheric composition and interior dynamics. The 75-day signal is less certain, being significantly affected by aliasing interactions among a potential 91-day signal, and the likely rotation period of the star at 105 days detected in two activity indices. GJ 667C is the common proper motion companion to the GJ 667AB binary, which is metal poor compared to the Sun. The presence of a super-Earth in the habitable zone of a metal poor M dwarf in a triple star system, supports the evidence that such worlds should be ubiquitous in the Galaxy.

Subject headings: stars: planetary systems, techniques: radial velocities, stars: individual GJ 667C

1. Introduction

The Doppler detection of extrasolar planets is achieved by measuring the periodic radial velocity variations induced in a star by the presence of orbiting low-mass companions. The Doppler signature of a gas giant planet with orbital parameters similar to Jupiter is about 10 m s^{-1} over a period of 11 years. By comparison, Earth’s reflex barycentric pull on the Sun corresponds to 8 cm s^{-1} . The most precise spectrographs can deliver long-term stability at the level of $1\text{--}3 \text{ m s}^{-1}$ (Mayor et al. 2011; Vogt et al. 2010). This precision is sufficient to detect candidates of a few Earth masses in tight orbits around low-mass stars (M dwarfs). A key requirement in reaching such accuracy is the extraordinary calibration of both the wavelength scales of the spectrum and the instrumental point-spread-function. The two most successful methods used to date are (1) the Iodine cell technique (Butler et al. 1996) and (2) the construction of stabilized spectrographs fed by optical fibers (Baranne et al. 1996).

In the first of these two approaches, the star’s light is passed through a transparent cell containing Iodine gas at low pressure. The absorption spectrum of Iodine is imprinted on the star’s light, tracing precisely the same optical path as encountered by the star light in traversing the spectrometer. The combined spectrum of the star and Iodine is then modeled

to obtain a simultaneous point-spread-function, wavelength and Doppler shift solution for the stellar spectrum (Butler et al. 1996). The stabilized spectrograph approach relies on the construction of a vacuum-sealed spectrometer fed with optical fibers that produces a fairly constant instrumental profile and long-term wavelength stability. Each night, stabilized spectrographs are calibrated in wavelength by feeding the light from a wavelength standard source (e.g., Th/Ar lamp) through the same fiber as the science targets. This approach is exquisitely implemented by HARPS installed on the European Southern Observatory 3.6-m telescope at La Silla Observatory (Pepe et al. 2003). HARPS is a cross dispersed echelle spectrograph with a resolving power of $\lambda/\delta\lambda=110\,000$, and over the years has demonstrated 1 m s^{-1} long-term stability (Pepe et al. 2011; Mayor et al. 2011).

Even though HARPS is probably the most precise astronomical spectrometer ever built, the Cross-Correlation Function (CCF) data analysis method that has been commonly used to analyze this data, is suboptimal in the sense that it does not exploit the full Doppler information in the stellar spectrum (Pepe et al. 2002). For this reason, instead of using the CCF RVs provided by the ESO archive, we use a least-square template-matching method to derive new RV measurements. Thanks to the instrumental stability and the excellent wavelength calibration provided by the HARPS-ESO data reduction software, the model required to match each observation to a high signal-to-noise-ratio (SNR) template only needs to include a Doppler offset and a multiplicative polynomial to correct for the flux variability across each echelle order. The template is obtained by co-adding all the spectra after a preliminary RV measurement is obtained using the highest SNR observation. The least-squares matching technique has been used on HARPS data before. An example are the RV measurements on GJ 1214 ($V=14.57$) used to derive the mass of the transiting super-Earth reported in Charbonneau et al. (2009). The performance and description of our software tool, HARPS-TERRA (Template Enhanced Radial velocity Re-analysis Application) on a representative sample of stars can be found in Anglada-Escudé & Butler (submitted).

2. Observations

One of the M dwarfs with many public HARPS spectra but no published detections is GJ 667C. The ESO archive contains 143 observations of this star obtained between June 2004 and October 2008. Typical exposure time is between 900 and 1500 seconds and the average signal-to-noise ratio (SNR) is 64 at 6100 Å. At a 2009 conference, a planet candidate orbiting this star was announced with a period P of ~ 7 days. Also recently, Bonfils et al. (2011) reported the detection of a plausible signal with $P \sim 28$ days similar to one of the candidates we report here. However, no detailed analysis nor any data were provided

therein. We use our new HARPS-TERRA software to derive new RV measurements on GJ 667C (Anglada-Escudé & Butler submitted). The root-mean-square (RMS) of these RVs is 3.89 m s^{-1} , which is significantly larger than the median internal precision ($\sim 1.1 \text{ m s}^{-1}$) and the typical RMS found on other stable M dwarfs (Bonfils et al. 2011). We found that the CCF RV measurements provided by the ESO archive were noisier ($\text{RMS} \sim 4.3 \text{ m s}^{-1}$) causing the signals reported in Section 4 to appear less significant. In order to obtain more secure detections, we obtained 21 new measurements with the Planet Finder Spectrograph (PFS) between August 2011 and October 2011. PFS is a cross-dispersed echelle spectrograph recently installed at the 6.5m Clay Magellan Telescope at Las Campanas Observatory, and uses the Iodine cell technique to obtain RV measurements at $1\text{--}2 \text{ m s}^{-1}$ precision (Crane et al. 2010).

GJ 667C has also been observed with HIRES/Keck (Vogt et al. 1994) using the Iodine cell method for just over a decade. Such long-time of observation should deliver tighter constraints on long period signals. However, in August 2004, the HIRES CCD array was replaced and the data obtained prior to this upgrade is of markedly inferior quality. Post-fix HIRES measurements show similar scatter to the HARPS and PFS RVs, so only 20 post-fix HIRES observations were used in our analysis. We emphasize that the signals discussed here were first detected using HARPS-TERRA measurements only, and that the contribution of the PFS and HIRES data were to improve the sampling cadence and increase the significance of the detections. All the RV measurements used in our analysis are given in the on-line version of the manuscript.

3. Properties of GJ 667C

According to Skiff (2010), GJ 667C (HR 6426 C) is classified as an M1.5 dwarf. The star is a common proper motion companion to the K3V+K5V binary GJ 667AB (HR 6426AB, Kron et al. 1957). At the distance to the system ($\sim 6.8 \text{ pc}$), the minimum physical separation between GJ 667C and GJ667 AB is $\sim 230 \text{ AU}$. The metallicity of GJ 667AB has been measured before (e.g. Perrin et al. 1988) and amounts to $[\text{Fe}/\text{H}] = -0.59 \pm 0.10$, meaning that the system is metal poor compared to the Sun. The same studies show that the GJ 667AB pair is well within the main sequence, indicating an age between 2 and 10 Gyr (e.g. Cayrel de Strobel 1981). The membership of GJ 667 to a Galactic population is unclear. Although its low metallicity points to a thick disk membership, its total velocity in the Galactic Local Standard of Rest is rather low ($44.6 \pm 1.5 \text{ km s}^{-1}$), which is characteristic of thin disk kinematics (see Figure 3 in Bensby et al. 2003). The most recent parameters of GJ 667AB can be found in Cvetkovic & Ninkovic (2011) and Tokovinin (2008). Using

the empirical relations given by Delfosse et al. (2000), the HIPPARCOS parallax of the GJ 667AB pair (van Leeuwen 2007) and K band photometry from 2MASS (Skrutskie et al. 2006), we derived a mass of $0.310 \pm 0.019 M_{\odot}$ for GJ 667C. The luminosity and effective temperature of GJ 667C are derived from the models in Baraffe et al. (1998) by assuming the aforementioned mass, metallicity and an age of 5 Gyr.

4. Orbital analysis

Keplerian orbital fits to the combined RV data were obtained using the SYSTEMIC interface (Meschiari et al. 2009), which allows the interactive least-squares adjustment of complex multiplanetary systems to several data sets. To determine whether there was a significant periodicity remaining in the data, we used a custom-made version of a least-squares periodogram (Cumming 2004) that adjusts a separate zero-point offset to each instrument (HARPS,PFS, and HIRES).

To quantify the significance of a new signal, we estimated its False Alarm Probability (FAP) empirically. We created 10^5 synthetic sets by randomly permutating the RV measurements over the same observing epochs (while retaining membership within each instrument). We then computed the periodogram of each synthetic set. A *false alarm* was identified when a synthetic data set produced a periodogram peak higher than the power of the signal under inspection. The number of false alarms was then divided by the number of simulations to derive the FAP, which was used as a measure of the probability that a spurious detection arised due to an unfortunate arrangement of the noise. This method is widely used to assess the likelihood of periodic signals and a detailed description can be found elsewhere (e.g., Cumming 2004). Since a few tens of M dwarfs have been intensively followed up at 1 m s^{-1} precision (Bonfils et al. 2011) and to minimize the chances of detecting a false positive, only signals with a FAP $< 1\%$ were added to the solution (dotted lines in Figure 1).

The first detected signal was an extremely significant periodicity at 7.2 days (see Figure 1). No false alarms were found in any of the 10^5 synthetic sets indicating a FAP $< 0.001\%$. The signal corresponds to a planet with a minimum mass ($M \sin i$) of $5.2 M_{\oplus}$ (GJ 667Cb) and a slightly eccentric orbit.

After subtracting a Keplerian solution for GJ 667Cb, a secular trend was the next most significant signal. The magnitude of the trend ($\sim 1.8 \text{ m s}^{-1} \text{ yr}^{-1}$) is compatible with the gravitational pull from the GJ 667AB pair (maximum value is $\sim 3.6 \text{ m s}^{-1} \text{ yr}^{-1}$) but could also be caused by an additional unseen long-period companion. The corresponding FAP of this signal is 0.055%, a very significant detection. A tentative solution with a period of 7000

days provides a slight improvement to the fit due to some curvature detected when combining HIRES+PFS measurements (see Figure 2). We estimate that one more year of observations is required to determine if the signal is due to an additional low mass companion or due to the gravitational pull of the GJ 667AB binary.

The next signal also has a very low FAP (0.034%), and implies a planet with a period of 28.15 days and $M \sin i \sim 4.5 M_{\oplus}$ (GJ 677Cc). Although the period is close to the lunar aliasing frequency (~ 27.3 days), the orbital phase coverage is complete thanks to the multi-year time-span of the observations. Because of its small amplitude, eccentric solutions cannot be ruled out (Shen & Turner 2008; O’Toole et al. 2009). A Monte Carlo Markov Chain analysis (Ford 2005) indicates that this eccentricity (with 98% confidence) must be less than 0.27. At a semi-major axis of 0.123 AU, the stellar flux S reaching the top of its atmosphere is 90% of the solar flux received by Earth (S_0). Using L and T_{eff} for the host star, the relations given in Kane & Gelino (2011) provide boundaries of the zone at which liquid water could exist on an Earth-like planet (also called liquid water habitable zone, or HZ). In the canonical model presented in Kasting et al. (1993) and updated in Selsis et al. (2007), the inner and outer boundaries depend on the fractional cloud coverage for the putative planet and are displayed as thick gray rectangles in Figure 3. Even though these limits are uncertain, GJ 667Cc comfortably falls in this HZ and also satisfies the empirical limits set by an uninhabitable Venus and a possibly habitable early Mars (Selsis et al. 2007). Let us remark that the ultimate capability of GJ 667Cc to support liquid water depends on properties that are not yet known (e.g, albedo, atmospheric composition and interior dynamics). Detailed studies using realistic climatic and geodynamical models (e.g., Heng & Vogt 2011; Wordsworth et al. 2011) are needed to better assess its chances of supporting life.

After fitting for GJ 667Cc, we found a group of candidate periodicities between 75 and 105 days. This time domain is strongly affected by aliases. For example, HARPS data alone favors a period of 91 days, which is uncomfortably close to a very clear signal detected in two activity indices (Section 5). When combining all the data, the 75-day periodicity had the lowest FAP (0.021%), indicating that such signal could not be ignored in the analysis. A tentative orbital solution assuming a circular orbit is given in Table 1. A putative super-Earth with $P \sim 75$ days could also support liquid water if its atmosphere contained high concentrations of CO_2 (e.g., GJ 581d in Wordsworth et al. 2011). We reiterate that, until more observations become available, this signal should be considered with due caution.

In a more thorough analysis (not presented here for brevity), we examined other orbital solutions with up to 4 signals at alternative periods (including, among others, signals at periods of 105, 120, and 33 days). All these attempts delivered significantly poorer fits, extreme eccentricities, and planetary systems that were unstable on time scales shorter than

1 Myr.

We also performed long-term N-body simulations based on some of our fits using the Hybrid symplectic integrator included in the Mercury integration package (Chambers 1999). We included the first order partial Post-Newtonian correction in the central star’s gravitational potential as in Lissauer & Rivera (2001) and used a time step of 0.2 days. We assumed a coplanar system throughout. Since the ratio of the periods of the inner two planets is near 4:1, we checked the four critical angles (involving only the periastron longitudes, ω) for the 4:1 mean motion resonance (MMR). We also examined the difference in the periastron longitudes. We found that the critical angles for the MMR circulate, whereas the difference in the longitudes of periastron librates about 180 deg with amplitude ~ 90 deg. Results of our simulations also show that the eccentricities of the planets librate between 0.0 and 0.235 for companion b and between 0.04 and 0.265 for companion c in opposite senses as a result of angular momentum conservation. Thus, the system appears to be protected by a secular resonance between the two inner planets in which 1) the orbits can become nearly anti-aligned when the eccentricity of b is small, and 2) the periastron longitudes are nearly perpendicular when the eccentricity of b is large. Most of the time, the system is in the second configuration (in good agreement with the fitted parameters in Table 1). This stabilizing mechanism appears to function for at least the first 25 Myr of our simulations. Further research into the dynamical evolution of this system is warranted once the nature of the other two signals (long-period trend and the 75/91-day candidate) is better understood.

5. Periodic signals in the activity indicators

Here we show the analysis of the time series of three activity indicators : the Bisector span (BIS), the full-width-half-maximum of the CCF (FWHM) and the CaII H+K S-index in the Mount Wilson system (S-index). Measurements of the BIS and the FWHM were provided by the HARPS-ESO pipeline. The S-index (Baliunas et al. 1995) was directly measured on the blaze-corrected spectra using the definitions given by Lovis et al. (2011). Since the BIS and FWHM could not be obtained in the Iodine cell approach, we limited our analysis to the HARPS observations only. Briefly, the BIS is a measure of the asymmetry of the average spectral line and should correlate with the RV if the observed offsets are caused by spots or plages rotating with the star (Queloz et al. 2001). The FWHM is a measure of the width of the mean spectral line and its variability is usually associated with changes in the convective patterns on the surface of a star. Lovis et al. (2011) found that the FWHM is the most informative index when investigating the correlation of stellar activity with RV variability on cool stars ($T_{eff} < 4600$ K). The S-index is an indirect measurement of the chromospheric

emission which depends upon the intensity of the stellar magnetic field. Because the strength of the magnetic field affects the efficiency of convection, the S-index could also correlate with observed RV variability. Since the connection between activity and RV jitter on M dwarfs is not well understood at the few m s^{-1} level (Lovis et al. 2011), we limit our analysis to evaluate if any of the indices has a periodicity that could be related to any of the detected candidates.

While the BIS did not show any significant periodicity, the S-index and especially the FWHM did show significant power around 105 days. To obtain meaningful periodograms, one outlier point had to be removed in the FWHM (a $9.4\text{-}\sigma$ outlier at $\text{JD}=2454677.66$) and another one from the S-index (a $13\text{-}\sigma$ outlier at $\text{JD}=2454234.79$). The FAPs of such signals were obtained by applying same empirical method used for the RVs. We found that the 105-day peak in the S-index had a FAP of 0.2% and no false alarms were found in any of the synthetic sets generated for the FWHM ($\text{FAP}<0.001\%$). Given the low metallicity and the age estimates of the GJ 667AB binary, GJ 667C should have a slow rotation rate (Irwin et al. 2011) compatible with the 105-day signal observed in these two indices. Because of the significant aliases affecting the ~ 100 -day time domain, it is likely (but not conclusive) that GJ 667Cd is a spurious signal resulting from localized magnetic activity rotating with the stellar surface. In addition to more RV observations to improve the phase sampling, a photometric follow-up could help to reveal the true nature of GJ 667Cd.

6. Conclusions

We have derived precision RV measurements from public HARPS spectra using a least-squares matching approach on the M dwarf GJ 667C and thereby detected the Doppler signature of (at least) two planets. Additional observations with PFS and HIRES confirm the detection of these signals and further constrain the orbital parameters. Even though the public CCF Doppler measurements are not as precise, the CCF method still provides useful information on stellar activity that can be used to investigate the origin of candidate signals.

GJ 667Cc is the super-Earth candidate most securely detected within the liquid water habitable zone of another star. As for other proposed candidates (e.g., GJ 581d and HD 85512b announced in Mayor et al. 2009; Pepe et al. 2011, respectively), its actual capability of supporting liquid water depends on many physical properties that are yet unknown. Using the relations given by Charbonneau et al. (2007), the reported candidates have non-negligible probabilities of transiting in front of the star ($\sim 2.7\%$, 1.1% , and 0.6% for planets b, c, and d, respectively). Even though these probabilities are low, the estimated transit depth assuming a density similar to Earth, is about 0.3% , which can be measured using small aperture

telescopes. Statistical extrapolations based on Doppler, transit and microlensing surveys indicate that such planets should be abundant around main sequence stars (Mayor et al. 2009; Borucki et al. 2011; Cassan et al. 2012). With the new generation of optical and infrared spectrographs, many nearby M dwarfs will be efficiently surveyed for low mass planets. If the detection rate holds, very soon now we may have a real chance of searching for spectroscopic signatures of water and life on one of these worlds.

Acknowledgements We thank the constructive comments given by the anonymous referee. This research has been partially supported by the Carnegie Postdoctoral Program to GAE; ICM P07-021-F, FONDAF 15010003 and BASAL-CATA PFB-06 grants to DM and PA; NSF grant AST-0307493 to SSV; NASA NNX07AR40G and NASA Keck PI program grants to RPB; NASA grants NNA04CC08A and NNX09AN05G to NH; ARC grant DP774000 to CGT; and Fondecyt grant 3110004 to JSJ. This work is based on data obtained from the ESO Science Archive Facility. Observations were obtained from Las Campanas Observatory and W. M. Keck Observatory. W. M. Keck Observatory is operated jointly by Univ. of California and California Institute of Technology. This research has made use of the SIMBAD database, operated at CDS, Strasbourg, France.

REFERENCES

- Anglada-Escudé, G., & Butler, R. P. submitted to ApJS, –,
Baliunas, S. L., Donahue, R. A., Soon, W. H., et al. 1995, ApJ, 438, 269
Baraffe, I., Chabrier, G., Allard, F., & Hauschildt, P. H. 1998, A&A, 337, 403
Baranne, A., et al. 1996, A&AS, 119, 373
Bensby, T., Feltzing, S., & Lundström, I. 2003, A&A, 410, 527
Bonfils, X., Delfosse, X., Udry, et al. 2011, e-prints arXiv:1111.5019
Borucki, W. J., Koch, D. G., Basri, G., et al. 2011, ApJ, 736, 19
Butler, R. P., Marcy, G. W., Williams, E., et al. 1996, PASP, 108, 500
Cassan, A., Kubas, D., Beaulieu, J.-P., et al. 2012, Nature, 481, 167
Cayrel de Strobel, G. 1981, Bulletin d’Information du Centre de Données Stellaires, 20, 28
Chambers, J. E. 1999, MNRAS, 304, 793

- Charbonneau, D., Berta, Z. K., Irwin, J., et al. 2009, *Nature*, 462, 891
- Charbonneau, D., Brown, T. M., Burrows, A., & Laughlin, G. 2007, *Protostars and Planets V*, 701
- Crane, J. D., Shtetman, S. A., Butler, R. P., et al. 2010, in *SPIE Conference Series*, Vol. 7735
- Cumming, A. 2004, *MNRAS*, 354, 1165
- Cvetkovic, Z., & Ninkovic, S. 2011, *VizieR On-line Data Catalog: J/other/Ser/180.71*, 4201, 18001
- Delfosse, X., Forveille, T., Ségransan, D., et al. 2000, *A&A*, 364, 217
- Ford, E. B. 2005, *AJ*, 129, 1706
- Heng, K., & Vogt, S. S. 2011, *MNRAS*, 415, 2145
- Irwin, J., Berta, Z. K., Burke, C. J., et al. 2011, *ApJ*, 727, 56
- Kane, S. R., & Gelino, D. M. 2011, *ApJ*, 741, 52
- Kasting, J. F., Whitmire, D. P., & Reynolds, R. T. 1993, *Icarus*, 101, 108
- Kron, G. E., Gascoigne, S. C. B., & White, H. S. 1957, *AJ*, 62, 205
- Lissauer, J. J., & Rivera, E. J. 2001, *ApJ*, 554, 1141
- Lovis, C., et al. 2011, *ArXiv e-prints*
- Mayor, M., Bonfils, X., Forveille, T., et al. 2009, *A&A*, 507, 487
- Mayor, M., Marmier, M., Lovis, C., et al. 2011, *ArXiv e-prints*
- Meschiari, S., Wolf, A. S., Rivera, E., et al. 2009, *PASP*, 121, 1016
- O’Toole, S. J., Tinney, C. G., Jones, H. R. A., et al. 2009, *MNRAS*, 392, 641
- Pepe, F., Mayor, M., Galland, et al. 2002, *A&A*, 388, 632
- Pepe, F., Rupprecht, G., Avila, G., et al. 2003, in *SPIE Conference Series*, Vol. 4841, 1045–1056
- Pepe, F., et al. 2011, *A&A*, 534, A58+

- Perrin, M.-N., Cayrel de Strobel, G., & Dennefeld, M. 1988, *A&A*, 191, 237
- Queloz, D., et al. 2001, *A&A*, 379, 279
- Selsis, F., Kasting, J. F., Levrard, B., et al. 2007, *A&A*, 476, 1373
- Shen, Y., & Turner, E. L. 2008, *ApJ*, 685, 553
- Skiff, B. A. 2010, *VizieR Online Data Catalog*, 10, 2023
- Skrutskie, M. F., et al. 2006, *AJ*, 131, 1163
- Tokovinin, A. 2008, *MNRAS*, 389, 925
- van Leeuwen, F. 2007, *A&A*, 474, 653
- Vogt, S. S., Allen, S. L., Bigelow, B. C., et al. 1994, in *SPIE Conference Series*, ed. D. L. Crawford & E. R. Craine, Vol. 2198, 362
- Vogt, S. S., Butler, R. P., Rivera, E. J., et al. 2010, *ApJ*, 723, 954
- Wordsworth, R. D., Forget, F., Selsis, F., et al. 2011, *ApJ*, 733, L48

Table 1. Best Keplerian solution to the planetary system around GJ 667C. The numbers in parenthesis indicate the uncertainty in the last two significant digits of each parameter value. Uncertainties have been obtained using a Bayesian MCMC analysis (Ford 2005) and represent the 68% confidence levels around the preferred solution. All orbital elements are referred to $JD_0 = 2453158.7643$. The properties of the star are listed at the bottom (references given in the text).

Parameter	b	c	(d?)	Trend
P [days]	7.20066(67)	28.155(17)	74.79(12)	7100(3000)
$M \sin i [M_{jup}]$	0.01789(75)	0.0143(12)	0.0178(17)	0.25(12)
$M \sin i [M_{\oplus}]$	5.68(23)	4.54(38)	5.65(54)	79(40)
M_0 [deg]	106.6(3.5)	144(25)	211(11)	231(10)
e	0.172(43)	<0.27	0(fixed)	0(fixed)
ω [deg]	344(12)	238(20)	0(fixed)	0(fixed)
Detection FAP	< 0.001%	0.034%	0.021%	0.055%
K [m s ⁻¹]	3.90	2.02	1.84	8.41
a [AU]	0.049	0.123(20)	0.235	2.577
S/S0	570%	90.5(3.0)%	24.8%	–
Statistics				
N_{HARPS}	143		Total N_{obs}	184
RMS_{HARPS} [m s ⁻¹]	1.89		RMS [m s ⁻¹]	2.05
N_{PFS}	21		χ^2	310.99
RMS_{PFS} [m s ⁻¹]	2.37		χ^2_{ν}	1.88
N_{HIRES}	20			
RMS_{HIRES} [m s ⁻¹]	2.85			
Star parameters		Derived quantities		
R.A.	17 18 57.16		Mass [M_{\odot}]	0.310(19)
Dec	-34 59 23.14		Spectral type	M1.5V
$\mu_{R.A.}$ [mas yr ⁻¹]	1129.7(9.7)		UVW _{LSR} [km s ⁻¹]	(19.5, 29.4,-27.2)
$\mu_{Dec.}$ [mas yr ⁻¹]	-77.02(4.6)		Age estimate	> 2 Gyr
Parallax [mas]	146.29(9.0)		T_{eff} [K]	3700±100
Hel. RV [km s ⁻¹]	6.5(1.0)		L_*/L_{\odot}	0.01370(90)
[Fe/H]	-0.59(10)		R_{in}^{HZ} [AU]	0.1145(72)
V [mag]	10.22(10)		R_{out}^{HZ} [AU]	0.226(14)
K [mag]	6.036(20)			

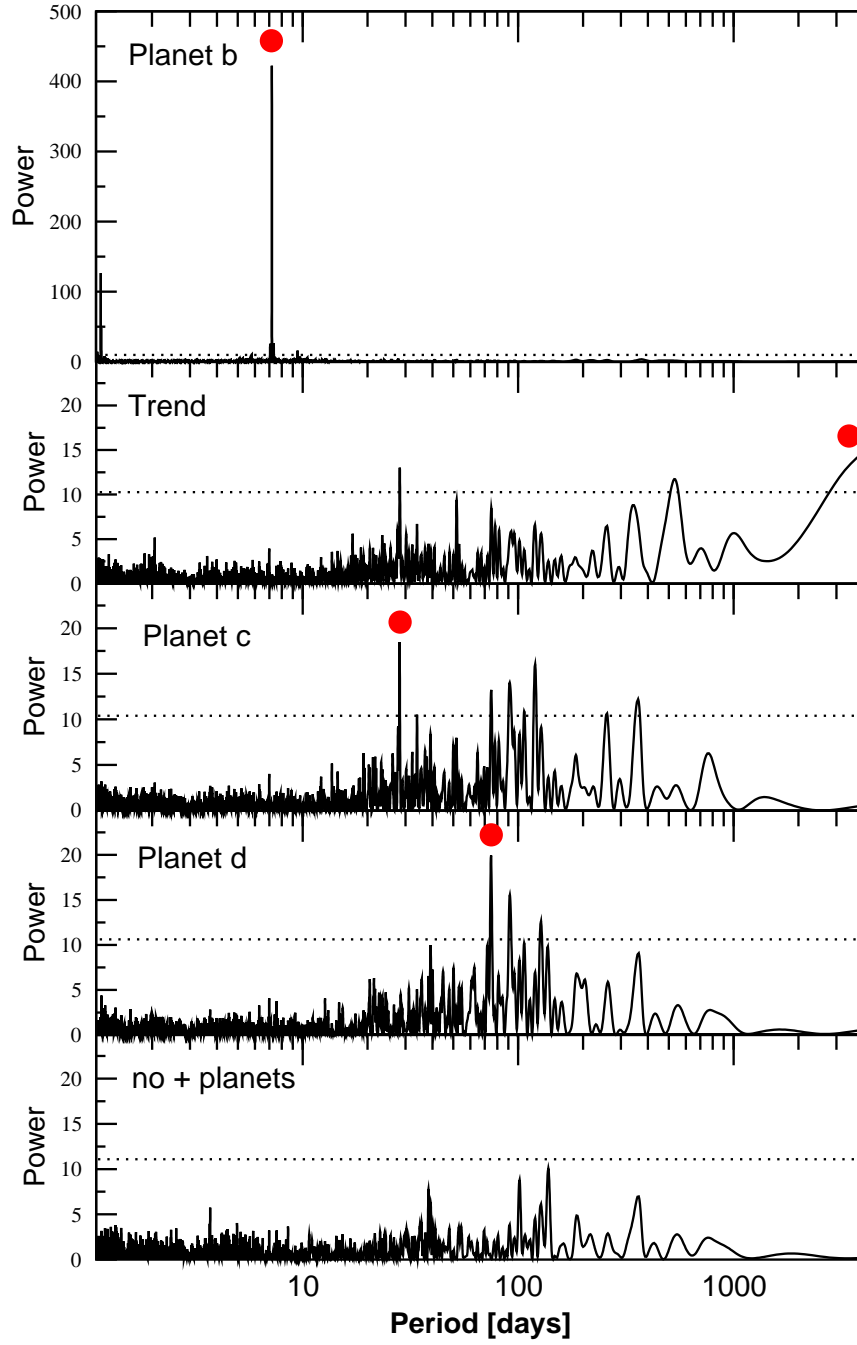


Fig. 1.— Detection periodograms of the three candidate planets and long period trend detected in the RV measurements of GJ 667C. The signals are listed from top to bottom in order of detection.

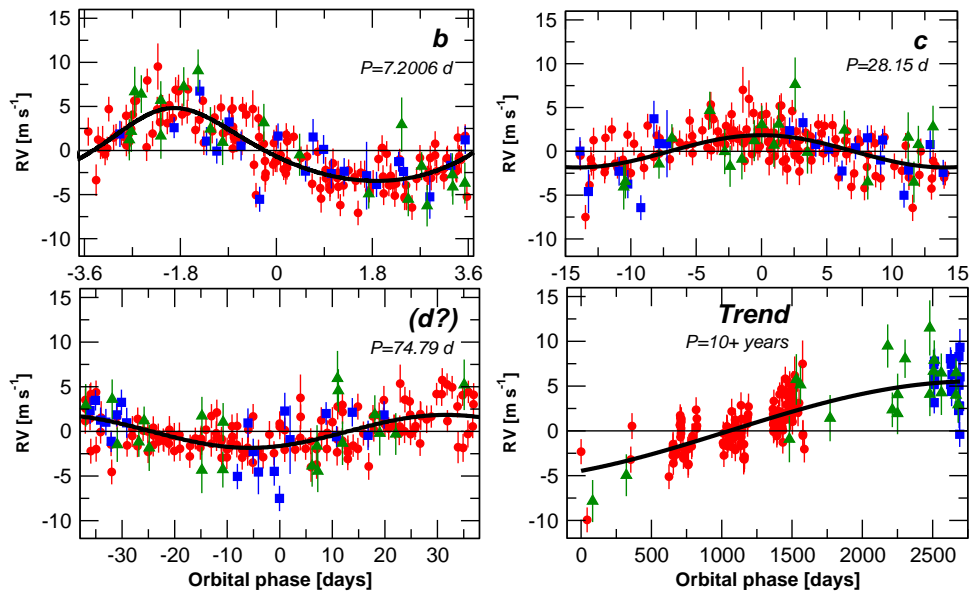


Fig. 2.— Phase-folded RV measurements of the four signals discussed in the text. The 143 HARPS measurements are shown in red circles, 21 PFS measurements are shown in blue squares and the green triangles correspond to the 20 HIRES observations. Each preferred Keplerian model is shown as a black line.

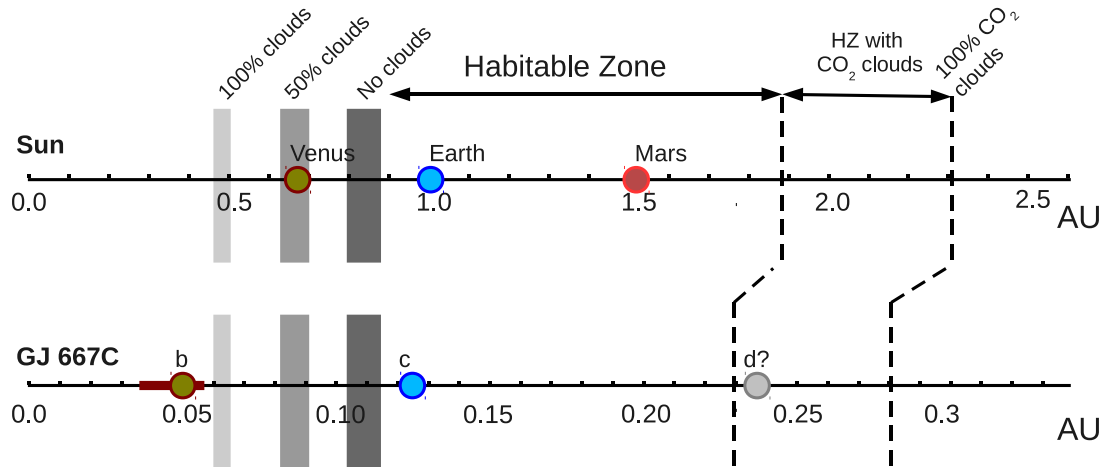


Fig. 3.— Comparative liquid water habitable zones for the Sun and GJ 667C (Selsis et al. 2007). The gray areas indicate the theoretical inner edge for different fractional cloud coverage. The outer edge is marked with a dashed line. The actual habitability of GJ 667C depends on physical parameters that are currently unknown.

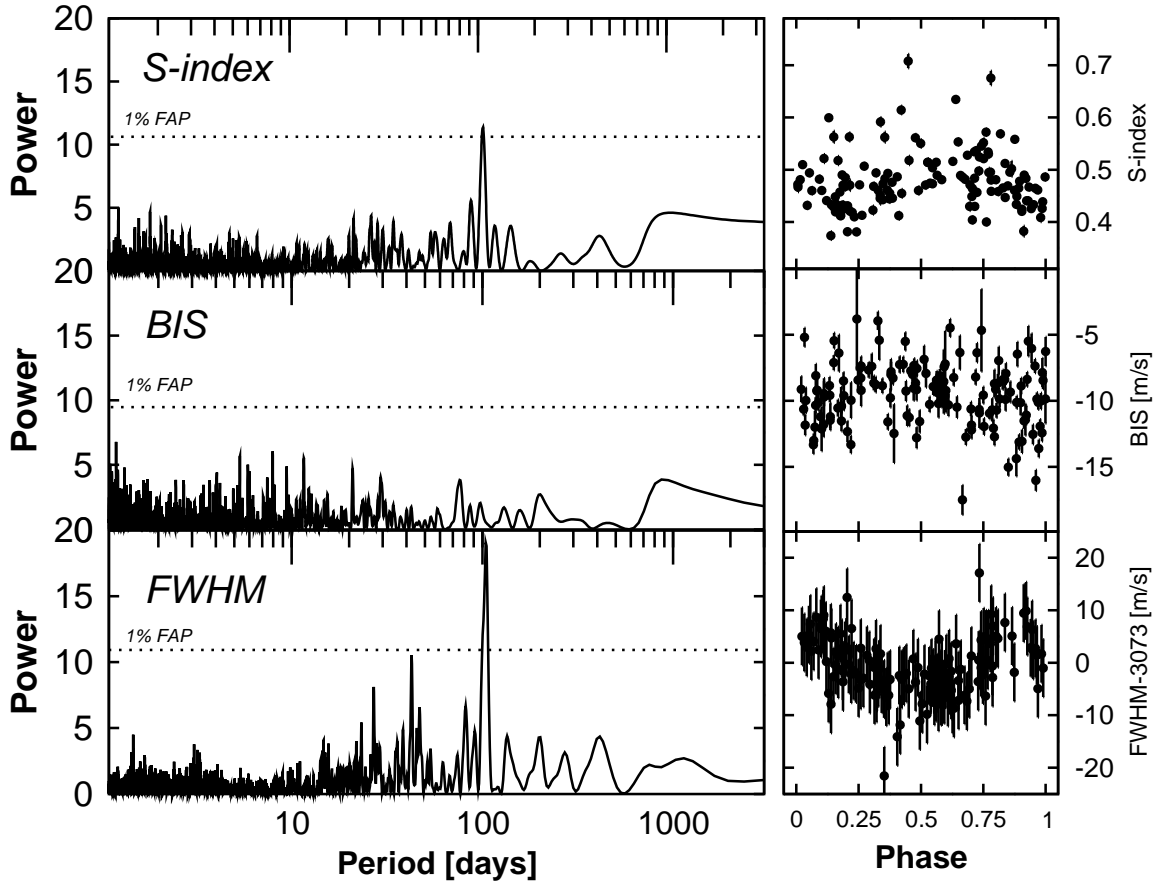


Fig. 4.— Left: Periodograms of the three activity indicators discussed in the text. Both the S-index and the FWHM show a significant signal around 105 days. On the right, we show each activity indicator folded to the most significant period : 105 days for the S-index and the FWHM, and 1.2008 days for the BIS.